Stellar dynamical evidence for dark halos in elliptical galaxies - The case of NGC 4472, IC 4296, and NGC 7144

Saglia, R.P.; Bertin, G.; Bertola, F.; Danziger, I.J.; Dejonghe, H.; Sadler, E.M.; ... ; Zeilinger, W.W.

STELLAR DYNAMICAL EVIDENCE FOR DARK HALOS IN ELLIPTICAL GALAXIES: THE CASE OF NGC 4472, IC 4296, AND NGC 7144[1]

R. P. SAGLIA
Landessternwarte, Königstuhl, D-6900 Heidelberg, Germany

G. BERTIN
Scuola Normale Superiore, Piazza dei Cavalieri 7, I-56126 Pisa, Italy

F. BERTOLA
Department of Astronomy, University of Padova, 35100 Padova, Italy

J. DANZIGER
European Southern Observatory, Karl-Schwarzschildstraße 2, D-8046 Garching bei München, Germany

H. DEJONGHE
R.U.G. Observatorium, Krijslaan 281, B-9000 Gent, Belgium

E. M. SADLER
Anglo-Australian Observatory, P.O. Box 296, Epping, New South Wales 2121, Australia

M. STIAVELLI
Scuola Normale Superiore, Piazza dei Cavalieri 7, I-56126 Pisa, Italy; and European Southern Observatory

P. T. DE ZEEUW
Sterrewacht, Postbus 9513, Leiden, 2300RA, The Netherlands

AND

W. W. ZEILINGER
European Southern Observatory, Karl-Schwarzschildstraße 2, D-8046 Garching bei München, Germany

ABSTRACT

Extended and accurate major axis kinematical profiles and line strength gradients of the elliptical galaxies NGC 4472, IC 4296, and NGC 7144 have been measured using the ESO NTT in the EMMI long-slit spectroscopic mode. For NGC 7144 the stellar rotation curve and velocity dispersion profile extend to 75″ from the center (where the surface brightness is 24.4 B-mag arcsec^{-2}, 2.8 mag below the sky), with typical error bars of 10 km s^{-1}. The flat or slowly increasing velocity dispersion profiles of these galaxies indicate that massive dark halos might dominate their dynamics.

Subject headings: galaxies: elliptical and lenticular, cD — galaxies: individual (IC 4296, NGC 4472, NGC 7144) — galaxies: kinematics and dynamics

1. INTRODUCTION

The velocity dispersion profiles of elliptical galaxies measured out to distances less than 1 R_e show a variety of shapes (Illingworth 1981), decreasing outward more or less slowly. One of the main results of the ESO Key Program "A Search for Dark Matter in Elliptical Galaxies" (Bertin et al. 1989) has been the discovery that the velocity dispersion profiles of a few selected objects, as measured out to very large distances from the center (about 2 R_e), are found to be decreasing outward relatively fast, in the way expected in the absence of dark matter. Indeed the modeling of these extended profiles, using two different approaches (Bertin, Saglia, & Stiavelli 1992, hereafter BSS; Dejonghe 1989), indicated that they are consistent with a mass distribution similar to that of the light. Therefore there seems to be no stringent need for invoking dark matter in the sampled regions (Bertin et al. 1991). This is in agreement with the results obtained for NGC 5077 (Bertola et al. 1991) using a gaseous disk as a probe of the galactic gravitational potential inside 1 R_e.

On the other hand, Efstathiou, Carter, & Ellis (1982, hereafter EEC) measured a nearly flat velocity dispersion profile for NGC 5813 out to 90″ (1.3 times the R_e derived from their photometric fit), and previous observations of NGC 4472 (Davies & Birkinshaw 1988, hereafter DB) extending only to about 0.5 R_e indicated a more slowly decreasing velocity dispersion profile. This has been interpreted as being due to the presence of a dark massive halo (EEC; Saglia, Bertin, & Stiavelli 1992, hereafter SBS).

In order to clarify the phenomenology of the velocity dispersion profiles *at large radii*, we decided to study more carefully some ellipticals which are known to have slowly decreasing velocity dispersion profiles in the inner regions. Our aim is to obtain reliable data reaching as far out as possible with state-of-the-art technology. The discovery that kinematic profiles do remain flat or even rise at large radii would yield substantial evidence for the presence of massive dark halos. Accordingly, in this paper we present the major axis kinematical profiles of NGC 4472, IC 4296, and NGC 7144. All these ellipticals are suspected of having a fairly flat velocity dispersion on the basis of previous observations.

In addition, based on the same spectroscopic data, we have measured radial absorption-line strength gradients for a

number of indices (Mg_1, Mg_2, Mgb, Fe5270, Fe5335). Since it has been claimed that color gradients are due to metallicity gradients (Peletier 1989) and that they correlate with a dynamical indicator that has been interpreted as the "local escape velocity" (Franx & Illingworth 1990, hereafter FI), it may be interesting to check whether objects with relatively flat velocity dispersion profiles have essentially constant abundances.

In § 2 the observational setup and the data reduction are described; the kinematical data derived with the Fourier Correlation Method (Bender 1990) are shown and discussed in § 3. Limits on the amount of dark matter implied by these observations are derived in § 4, and the possibilities to further improve and extend these results are examined in the Conclusions.

2. OBSERVATIONS AND DATA REDUCTION

Three objects have been selected among the brightest (round) elliptical galaxies observable from La Silla and extensively studied in the past, NGC 4472, IC 4296, and NGC 7144. Two of them (NGC 4472 and IC 4296) are well-known X-ray sources (Forman, Jones, & Tucker 1985; Canizares, Fabbiano, & Trinchieri 1987; Killeen, Bicknell & Carter 1986, hereafter KBC). NGC 4472 has been already indicated to possess an extended dark halo (SBS; see also Mould et al. 1990).

The observations were carried out during 1991 June 11–14, using the NTT and EMMI in the Red Medium Spectroscopy mode. The detector was the Ford CCD (ESO No. 24), with 2048×2048 15 μm pixels and a readout noise of 8 e^- per pixel. The EMMI grating No. 6 (28 Å mm^{-1}) was used in order to be able to use a large slit width (3″) and still have good resolution ($\sigma_{\text{instrum}} = 60$ km s^{-1}). The central wavelength was 5150 Å with 700 Å of spectral range.

In order to accumulate the maximum possible signal, repeated exposures of the galaxies were taken along the major axis only. The very long slit of EMMI (6′) allowed us to measure accurately the sky at one end of it, by putting the galaxies at the other end. We cumulated 5400 s of clear sky exposure for NGC 4472 (P.A. = 162°), 10,800 s for IC 4296 (P.A. = 60°), and 31,320 s for NGC 7144 (P.A. = 27°); eight velocity template stars and three spectrophotometric standards were also observed.

After the standard steps of data reduction (bias subtraction, division by the dome flat field, normalized along the wavelength direction and with slit function correction included, filtering of cosmic rays), the frames were calibrated in wavelength using Thorium comparison lamp spectra. The wavelength shift between comparison spectra taken before and after the scientific exposures is always less than the rms residual of the calibration (≈ 0.2 Å). The frames were rebinned in logarithmic steps using 800 pixels with a bin size of 50 km s^{-1}, covering the spectral range 4850–5550 Å. In this procedure flux was conserved in order to keep track of the original S/N ratio of the spectra. One-dimensional spectra were extracted from each frame of the velocity templates and of the spectrophotometric stars. No appreciable gradient in the spacial direction ($<2\%$) was present in the sky. Many rows (100–200) were averaged in order to derive a noise-free sky spectrum, starting from $\approx 180″$ from the centers of the galaxies. Even in the case of NGC 4472, where $R_e = 104″$, the sky portion of the slit is not too seriously contaminated by residual light from the galaxy (less than 5% of the value of the sky). After sky subtraction, the residuals in the sky lines at the opposite end of the slit were found to be consistent with Poisson noise.

The repeated exposures of the single galaxies were aligned and summed to produce a final frame for each galaxy (only one frame was available for NGC 4472). Finally, the summed frames were rebinned along the slit, by averaging contiguous rows in both directions from the centers separately, until a fixed S/N ratio (≥ 15) was reached. The minimum step size was set to 1″.05. The most distant bins have the lowest S/N ratios. The luminosity-weighted distance from the center was assigned to each obtained spectrum. In the case of IC 4296 a star superposed on one side of the galaxy was masked before the rebinning was applied.

The spectra of the template stars and of the rebinned frames of the galaxies were continuum divided and edge-masked with a cosine bell function. The resulting spectra were analyzed using the Fourier Correlation Quotient Program (Bender 1990), to derive the radial velocity curves and the velocity dispersion profiles of the three galaxies. HD 208817 was used as template; use of other template stars caused insignificant changes in the derived kinematic data.

A detailed test was performed in order to verify the effects of our sky subtraction procedure on the final kinematical profiles and in particular of the oversubtraction due to contamination with residual galactic light. Systematic effects due to sky subtraction errors alone were found to be small (less than 10 km s^{-1} in σ; see EEC). Oversubtraction of the sky produced velocity dispersion larger than the true values. The (larger) effect caused by the oversubtraction due to galactic light contamination was estimated as follows. A simulated frame of a galaxy was produced, by broadening the spectrum of a template star with a velocity dispersion profile given by $\sigma(R)[\text{km s}^{-1}] = \sigma_0 \times [1 + \alpha \times R]$, where R is the distance from the center in arcseconds, $\sigma_0 = 200$, 300 km s^{-1}, and $\alpha = 0, \pm 0.0033$ arcsec^{-1}. The number of counts along the slit was scaled using an $R^{1/4}$ law with given R_e, and Poisson noise was added. A simulated sky frame was computed, using the noise-free sky spectrum determined from one of the long exposures of NGC 7144, adding Poisson noise and Gaussian readout noise. The simulated frames of the galaxy and of the sky were added and analyzed using the procedures adopted for the galaxy frames. A template star different from the one adopted to generate the simulated galaxy was used in the FCQ analysis. The derived velocity dispersions were systematically larger (smaller) than the true values, if the decreasing, $\alpha < 0$ (increasing, $\alpha > 0$) profile was considered. However, the size of the effect becomes relevant only when the oversubtraction is a consistent fraction of the signal. For example, using $R_e = 40″$ and $\sigma_0 = 200$ km s^{-1} (as in the case of NGC 7144), the oversubtraction at 2 R_e amounts to 20% of the signal. The resulting σ is ≈ 20 km s^{-1} larger than the true value in the case of a decreasing profile.

Finally, we obtained radial line-strength indices for Mg_1, Mg_2, and Mgb, Fe5270, and Fe5335 as defined by Burstein et al. (1984). The galaxy spectra were normalized to an absolute flux scale using the spectra of the spectrophotometric standard stars. Uncertainties regarding the flux calibration were found to affect only the zero point of the indices but not the line strength gradients. The iron indices are affected by broadening due to the velocity dispersion. Correction factors to the Fe5270 and Fe5335 indices were applied as a function of the amount of velocity dispersion using the relation given by Gorgas, Efstathiou, & Salamanca (1990, hereafter GES). An independent check was performed by convolving stellar spectra with appropriate Gaussians. The derived correction factors are found to be in good agreement with those obtained from GES. In order

DARK HALOS IN ELLIPTICALS

to improve the S/N ratio the galaxy spectra were resampled in 5″ intervals.

3. OBSERVATIONAL RESULTS

In Figure 1 the velocity dispersion profiles, radio velocity curves, and Mg_2 and $\langle Fe \rangle = (Fe5270 + Fe5335)/2$ line strength profiles for NGC 4472, IC 4296, and NGC 7144 are presented. The mean velocity inside the inner 5″–10″ has been subtracted from the radial velocities, and the profiles have been folded with respect to the centers of the galaxies. Both the stellar rotation curve and the velocity dispersion profile are symmetric with respect to the center even at the outermost points. The error bars are typically less than 15 km s^{-1} and somewhat larger at the largest distances, where the spectra have relatively a low S/N ratio. We discuss each galaxy in turn.

NGC 4472.—The kinematical data extend to a distance that is almost twice the distance of the previously available measurements, reaching 1 R_e at a surface brightness of 23 B arcsec^{-2}. Comparison with major axis data for the inner 50″ of

DB gives a relative rms scatter of 22 km s^{-1} in velocity dispersion, mainly due to differences in the outer parts, where DB's data are about 50 km s^{-1} lower, and of 14 km s^{-1} in the stellar rotational velocities. The counterrotating stellar core of the galaxy (DB) is clearly visible in the inner 6″, while the slowly decreasing velocity dispersion profile nicely matches the data derived from globular cluster kinematics (Mould et al. 1990). If one rebins the frame to obtain a lower S/N ratio, there are indications that the rotation curve may stay flat at the value of 80 km s^{-1} out to 150″ from the center.

IC 4296.—This is the most distant galaxy of the sample; all the frames collected for this object were obtained through some clouds. As a consequence, the derived kinematics extend only up to 45″ from the center ($\approx 0.8\ R_e$). A comparison with the data of Franx, Illingworth, & Heckman (1989a, hereafter FIH), gives relative rms of 21 km s^{-1} in σ and of 13 km s^{-1} in the stellar rotational velocities; higher scatter is observed with the less accurate values of KBC. In the inner 5″ the data confirm the peculiar kinematics already discovered by these
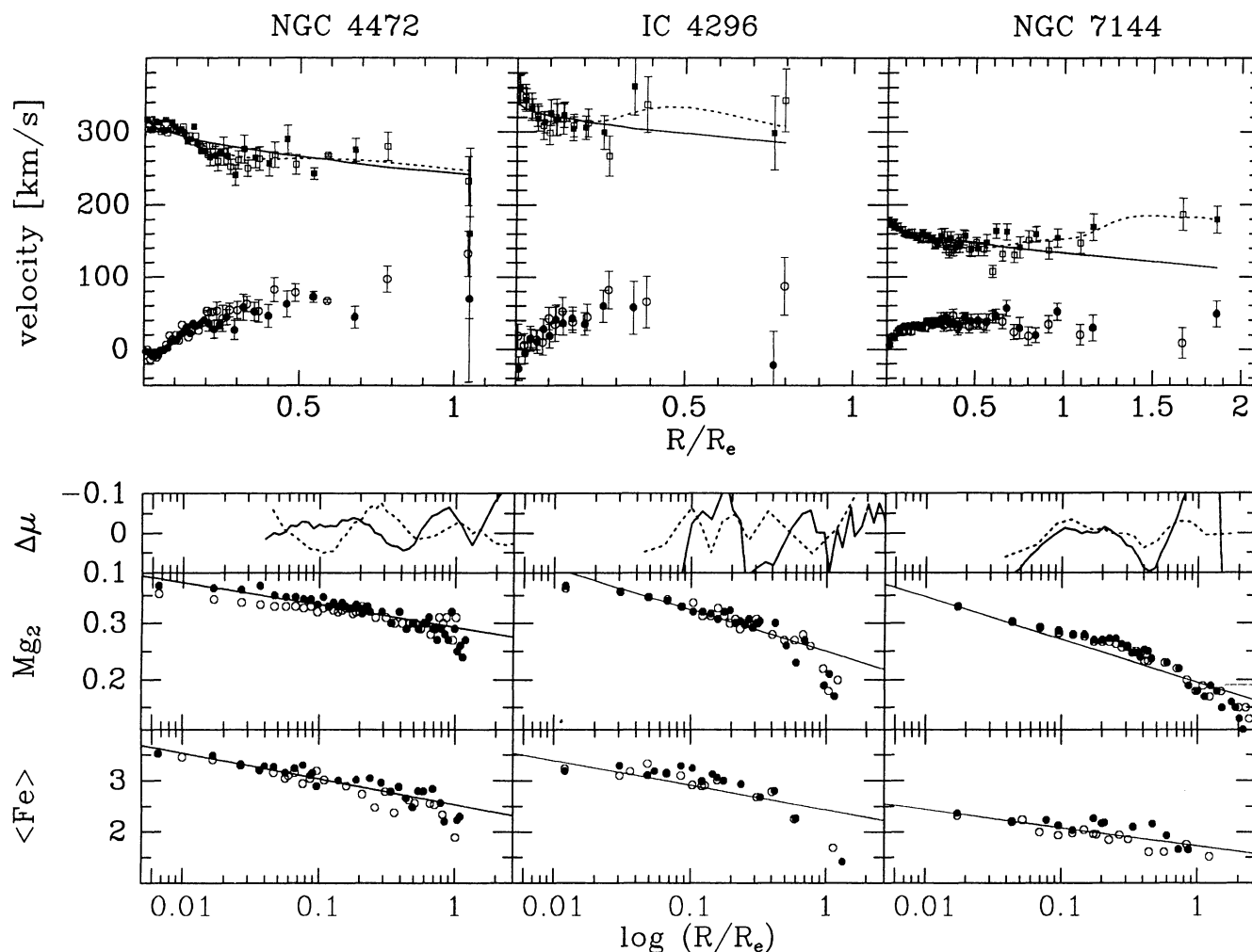

FIG. 1.—*Top panel*: Kinematical profiles along the major axis of NGC 4472 ($R_e = 104″$; Faber et al. 1989), IC 4296 ($R_e = 57″$; Faber et al. 1989), NGC 7144 ($R_e = 40″$; Faber et al. 1989). Dots represent radial velocity, and squares velocity dispersion data. Open and closed symbols refer to the two sides of the galaxies. The profiles have been folded with respect to the centers of the galaxies. The full lines show the velocity dispersion profiles of the best-fit two-component models, while the dashed lines those of the best-fit QP models (*see text*). *Lower panel, top*: residuals $\Delta\mu = \mu - \mu_{mod}$ between the surface brightness profiles in magnitudes and the projected densities of the luminous components of the best-fit two-component models (*full lines*) and of the best-fit QP models (*dashed lines*). *Middle*: Mg_2 line strength profile. Open and closed symbols refer to the two sides of the galaxies. The full lines show the fitted gradients. *Bottom*: $\langle Fe \rangle = (Fe5270 + Fe5335)/2$ line strength profile. Open and closed symbols refer to the two sides of the galaxies. The full lines show the fitted gradients.

authors and by FIH. Even in this case the kinematical profiles are fairly flat out to the outermost data point.

NGC 7144.—The kinematical profiles extend out to 75" from the center (2 R_e, 4 times the distance reached by the previously available data, FIH), at a surface brightness of 24.4 B arcsec^{-2} (Jedrzejewski 1987), 2.8 mag below the sky. Comparison with FIH data shows good agreement in the inner 15", with a relative rms in the velocity dispersion of 17 km s^{-1} and of 10 km s^{-1} in the stellar rotational velocities. The velocity dispersion profile rises slowly, and the rotation curve is nearly flat. After sky subtraction the flux at the two outermost data points is 0.6 mag fainter than the value derived from the photometry. Therefore the light "oversubtracted" amounts to $\approx 40\%$ of the signal. We expect half of this 40% to be due to the contamination of the sky with residual galactic light (see § 2). A 1%–2% error in sky subtraction can account for the remaining 20%. Following § 2, the velocity dispersions of the two outermost points could be ≈ 20 km s^{-1} (one error bar) larger than the true values, if the velocity dispersion at $R > 2$ R_e is decreasing.

Line-strength gradients.—The derived line strength gradients for NGC 4472 are $\Delta Mg_2/\Delta \log r = -0.04$, and $\Delta \langle Fe \rangle / \Delta \log r = -0.5$. All indices are symmetric with respect to the center except Mg_2 which shows an asymmetry with 10" from the center. For IC 4296 we derive $\Delta Mg_2/\Delta \log r = -0.074$ and $\Delta \langle Fe \rangle / \Delta \log r = -0.48$, and for NGC 7144 $\Delta Mg_2/\Delta \log r = -0.076$ and $\Delta \langle Fe \rangle / \Delta \log r = -0.36$. Line strength gradients are available in the literature for NGC 4472 (Boronson & Thompson 1991; GES) and IC 4296 (GES). These data, however, do not have much radial extent, and the derived gradients appear very noisy. Our central values are in good agreement with the published ones. In the outer parts, on the contrary, there is considerable scatter, although there seems to be agreement on the global trend.

4. DYNAMICAL MODELING

In this section we explore the stellar dynamical evidence for the presence of significant amounts of dark matter in the galaxies that we have observed. In the following analysis we have adopted the luminosity profiles derived by Peletier et al. (1990) and Michard (1985) for NGC 4472, the extended photometry derived by Marston (1988) for IC 4296, and the R-band CCD profile derived by Franx, Illingworth, & Heckmann (1989b) for NGC 7144. The zero points of the profiles have been adjusted to match the total B-magnitudes measured by Faber et al. (1989).

We have adopted a two-pronged modeling approach for the interpretation of the stellar dynamical data. On the one hand we use two-component self-consistent spherical nonrotating models based on anisotropic distribution functions of Maxwellian type multiplied by a weight factor of the form $(-E)^{3/2}$, with E the binding energy of the stars or the dark matter. These models originate from the physical picture of dissipationless collapse that envisages that elliptical galaxies are well relaxed, that is, with isotropic pressure inside R_e, and only incompletely relaxed, with a modest excess of radial orbits, in the outer regions (see, e.g., van Albada 1982). The presence of the dark component modifies the stellar kinematical profile with respect to the one that would be expected if the galaxy had a constant M/L. The models have been found to be a useful tool in the luminous-dark matter decomposition for elliptical galaxies (see BSS and SBS for further details). On the other hand, we also apply a quadratic programming (QP) method, which approx-

imates the spherical and nonrotating distribution function as a linear combination of simple components, for which we choose powers of E and of the total angular momentum J (Dejonghe 1989). See this paper, BSS, and SBS for a more extended discussion of alternative modeling procedures, such as the one devised by Binney & Mamon (1982). The QP method complements the first one, in that it makes fewer assumptions about the form of the distribution function and hence allows a larger freedom in the radial density profile and in the anisotropy of the velocity distribution. Both methods go beyond the simple analysis based on Jeans equations (see, e.g., EEC), since they determine the best-fit distribution function to the photometry and the kinematics of the galaxies. Our analysis ignores the rotation of the stars, since this is probably dynamically unimportant. In any case, including this contribution (see van der Marel, Binney, & Davies 1990; van Marel 1991) would strengthen our conclusion that dark halos are present around NGC 4472, IC 4296, and NGC 7144. Our modeling is based on spherically symmetric distribution functions. However, tests performed on flattened models (see SBS) show that for intrinsically nonspherical objects seen round in projection, the fitting method seems to underestimate the amount of dark matter present.

The models determined with these procedures and that best fit the photometry and the kinematics of the three galaxies under study are shown in Figure 1. The new extended kinematical data for NGC 4472 confirm the predictions of the best-fit two-component model selected by SBS, with $M_L/L_B = 5.9$ for the luminous component and a total $(M/L_B)_{R_e}$ ratio inside R_e of 8.9 (distance 22 Mpc). The *global* ratio is $M/L_B = 15.8$. In this case dark matter is found to be necessary, and we obtain a minimum value for the dark-to-luminous mass ratio of $M_D/M_L = 1.4$, when a "3 σ" cut is applied (see SBS). In this framework, one-component models (i.e., without dark matter), excluded by SBS at "7 σ", are now excluded at "12 σ". A similar result is obtained in the case of IC 4296, where the derived M_L/L_B for the luminous component is 5.6, while the total $(M/L_B)_{R_e}$ ratio inside R_e is 9.1 (distance 75 Mpc). The *global* ratio is $M/L_B = 32.8$. On the other hand, if one follows the more conservative approach (Dejonghe 1989), as to the problem of dark matter, of imposing a constant mass-to-light ratio and of postponing the problem of the physical justification of the phase space structure, then one finds that NGC 4472 and IC 4296 can indeed be modeled. Not surprisingly (see Tonry 1983) the best-fitting models have a tangentially biased pressure tensor [$\sigma_\theta/\sigma_r(0.2 \ R_e) = 1.5$, $\sigma_\theta/\sigma_r(R_e) = 2.6$ for NGC 4472, $\sigma_\theta/\sigma_r(0.2 \ R_e) = 1$, $\sigma_\theta/\sigma_r(R_e) = 1.6$, for IC 4296], which supports the nearly flat velocity dispersion profile. Still, these models require fairly large mass-to-light ratios ($M/L_B = 14$ and $M/L_B = 16$, respectively, adopted distances $D = 22$ Mpc and $D = 75$ Mpc). Note that these values essentially match the *total M/L* ratios obtained by the modeling with dark matter described above. A model with a completely tangential orbital structure, as the one proposed by Mould et al. (1990) for NGC 4472, would still give for this galaxy $M/L_B = 9$, about twice the value derived for the core.

The case of NGC 7144 is more complex, since for the first time a rising velocity dispersion profile at large radii (but see discussion in § 3) is observed in an elliptical that is not a cD (Dressler 1979; Carter et al. 1981, 1985) and does not show signs of recent interaction events (the nearest object is NGC 7145 at 22'.6, or 243 kpc with $D = 37$ Mpc). The two-component modeling of BSS (which however did not fully

explore the possibility of hot diffuse halos) gives unsatisfactory fits (see Fig. 1), as it is unable to reproduce the slowly rising part of the velocity dispersion profile. The best-fit model has in any case a massive dark halo with $M_D/M_L = 3.4$. The QP method fails also to construct a model with constant M/L that reproduces the rising velocity dispersion. Figure 1 shows a QP model derived allowing for the inclusion of dark matter. The model gives a very good fit to the data and has a massive dark halo, with $(M/L_B)_{2R_e} = 10$ and $(M_D/M_L)_{2R_e} = 2$. However, it might be difficult to imagine a formation process that would produce its very tangentially anisotropic orbital structure $[\sigma_\theta/\sigma_r(0.2\ R_e) = 1,\ \sigma_\theta/\sigma_r(2\ R_e) = 6]$. An increasing velocity dispersion profile could also result from the superposition of an inner component (e.g., a face-on disk) to an outer, hotter one. In any case, $M/L_B = 10$ is a *lower limit* to the amount of mass present in this galaxy: in the case of pure tangential orbits at $2\ R_e$, the circular velocity V_c must be greater than $\sqrt{2}\,\sigma(2\ R_e)$, and therefore $(M/L)_{2R_e} = (2\ R_e)V_c^2/(GL_{2R_e}) > 4\ R_e\,\sigma^2(2\ R_e)/(GL_{2R_e}) = 9.5$.

5. CONCLUSIONS

We have presented accurate kinematical and line strength profiles of NGC 4472, IC 4296, and NGC 7144 extending out to very faint surface brightness levels (24.4 B arcsec^{-2} in the case of NGC 7144). The dynamical modeling gives strong evidence for the presence of dark matter in these objects. In the cases of NGC 4472 and IC 4296 even the models characterized by a constant M/L ratio yield high values of M/L, consistent with those models that include a diffuse dark halo. Future measurements of the velocity dispersion profile of these two galaxies at larger distances from the center may remove the remaining ambiguity on M/L. For NGC 7144 we derive $(M_D/M_L)_{2R_e} = 2$ with an extremely tangentially anisotropic distribution of stellar orbits.

Is it possible to tentatively speculate about trends in the "global properties" of dark halos around ellipticals? So far we have collected fairly accurate kinematical data for a sample of nine objects (the three of this work and the six from Bertin et al. 1991). These indicate that some galaxies possess flatter velocity dispersion profiles than others beyond 1 R_e. Environmental effects seem to be unimportant, because both isolated and cluster galaxies can show flat or decreasing velocity dispersion profiles. We might expect that, if all dark halos had the same size (mass and scale length), these halos would have less effect on smaller galaxies, which should therefore in general be characterized by steeper dispersion profiles. This correlation is partly suggested by our data; a better correlation is probably with the average brightness inside 1 R_e, a distance-independent quantity. However, indications of this kind should be taken with caution, since the number of objects where the modeling is satisfactory is even smaller than nine.

For all our objects the derived Mg$_2$ and $\langle$Fe$\rangle$ line strength gradients extend at least to 1 R_e. The average ratio of Fe to Mg$_2$ gradients for our galaxies is significantly larger than that derived for the nuclei of ellipticals (Burstein et al. 1984), that is, $\Delta\langle$Fe$\rangle/\Delta$Mg$_2 \simeq 8.3 \pm 4$ compared to $\Delta\langle$Fe$\rangle/\Delta$Mg$_2 \simeq 2.6$. This agrees with Peletier's (1989) conclusion based on less extended and less accurate profiles. This suggests that the mechanism producing gradients in a galaxy is not the same as the one producing different abundances in different galaxies. It is hard to interpret this result theoretically, given the lack of a reliable calibration of indices with abundances. It should be noted, however, that dynamical effects during galaxy formation can strongly influence abundance gradients. Stiavelli & Matteucci (1991) find that Δ[Fe/H]$/\Delta$[Mg/H] varies by a factor 3 due to the dynamical effects only, that is, for a fixed initial gas mass and IMF, and it is larger in models with dark matter, in agreement with the conclusions of our dynamical modeling. The relation between line strength gradients and velocity dispersion profiles is not obvious; however, we find that flat velocity dispersion profiles do not imply flat abundance gradients.

It is possible to improve the results shown in this paper? The limiting factor of the present observational setup is still the readout noise of the CCD. This is the dominant contribution to the noise in the outer parts of an elliptical, since the electrons due to the sky in 2 hours of integration during dark time amount to ~ 40 per pixel, and the total amount of light passing through the slit at distances greater than 2 R_e is only 2% of the light collected at shorter distances. In fact, in the case of NGC 7144 all the rows at distances greater than 2 R_e added together to derive the last data point of Figure 1 have *decreased* the S/N ratio of the resulting spectrum. Adding together all the rows from $R = 80''$ to $R = 141''$ would produce a spectrum at a distance of 103'' (2.5 R_e), but with a S/N ratio of 3.4, too low to give accurate kinematical data. Nevertheless, it would be sufficient to bin together 10 pixels of the CCD during the observations or to use a CCD with a lower readout noise (1 electron per pixel) to decrease drastically the effect of the readout noise: the same radial range would now give a spectrum with S/N = 15. In this case the sky becomes the dominant source of noise. With such a setup, it should be possible to derive accurate kinematical data up to 3 R_e with 8 hours of integration time for all the three galaxies considered here, since all of them have approximately the same surface brightness at R_e ($\mu_B \approx 23\ B$ arcsec^{-2}).

REFERENCES

Bender, R. 1990, A&A, 229, 441
Bertin, G., et al. 1989, ESO Messenger, 56, 19
———. 1991, Proc. 2d DAEC Meeting, The Distribution of Matter in the Universe, in press
Bertin, G., Saglia, R. P., & Stiavelli, M. 1992, ApJ, 384, 423 (BSS)
Bertola, F., Bettoni, D., Danziger, I. J., Sadler, E. M., Sparke, L. S., & de Zeeuw, P. T. 1991, ApJ, 373, 369
Binney, J., & Mamon, G. A. 1982, MNRAS, 200, 361
Boronson, T. A., & Thompson, I. B. 1991, AJ, 101, 111
Burstein, D., Faber, S. M., Gaskell, C. M., & Krumm, N. 1984, ApJ, 287, 586
Canizares, C. R., Fabbiano, G., & Trinchieri, G. 1987, ApJ, 312, 503

Carter, D., Efstathiou, G., Ellis, R. S., Inglis, I., & Goodwin, J. 1981, MNRAS, 195, 15P
Carter, D., Inglis, I., Ellis, R. S., Efstathiou, G., & Goodwin, J. 1985, MNRAS, 212, 471
Davies, R. L., & Birkinshaw, M. 1988, ApJS, 68, 409 (DB)
Dejonghe, H. 1989, ApJ, 343, 113
Dressler, A. 1979, ApJ, 231, 659
Efstathiou, G., Ellis, R. S., & Carter, D. 1982, MNRAS, 201, 975 (EEC)
Faber, S. M., Wegner, G., Burstein, D., Davies, R. L., Dressler, A., Lynden-Bell, D., & Terlevich, R. J. 1989, ApJS, 69, 763
Forman, W., Jones, C., & Tucker, W. 1985, ApJ, 293, 102

Franx, M., & Illingworth, G. 1990, ApJ, 359, L41 (FI)
Franx, M., Illingworth, G., & Heckman, T. 1989a, ApJ, 344, 613 (FIH)
———. 1989b, AJ, 98, 538
Gorgas, J., Efstathiou, G., & Aragón Salamanca, A. 1990, MNRAS, 245, 217
    (GES)
Illingworth, G. 1981, in The Structure and Evolution of Normal Galaxies, ed.
    S. M. Fall & D. Lynden-Bell (Cambridge: Cambridge Univ. Press), 27
Jedrzejewski, R. I. 1987, MNRAS, 226, 747
Killeen, N. E. B., Bicknell, G. V., & Carter, D. 1986, ApJ, 309, 45 (KBC)
Marston, A. P. 1988, MNRAS, 230, 97
Michard, R. 1985, A&AS, 59, 205

Mould, J. R., Oke, J. B., de Zeeuw, P. T., & Nemec, J. M. 1990, AJ, 99, 1823
Peletier, R. 1989, Ph.D. thesis, Univ. Groningen
Peletier, R. F., Davies, R. L., Illingworth, G. D., Davis, L. E. & Cawson, M. C.
    1990, AJ, 100, 1091
Saglia, R. P., Bertin, G., & Stiavelli, M. 1992, ApJ, 384, 433 (SBS)
Stiavelli, M., & Matteucci, F. 1991, ApJ, 377, L79
Tonry, J. L. 1983, ApJ, 266, 58
van Albada, T. S. 1982, MNRAS, 201, 939
van der Marel, R. P. 1991, MNRAS, 253, 710
van der Marel, R. P., Binney, J., & Davies, R. L. 1990, MNRAS, 245, 582